

Breakdown of traditional many-body theories for correlated electrons

O. Gunnarsson,¹ G. Rohringer,^{2,3} T. Schäfer,² G. Sangiovanni,⁴ and A. Toschi²

¹ *Max-Planck-Institut für Festkörperforschung, Heisenbergstraße 1, D-70569 Stuttgart, Germany*

² *Institute of solid state physics, Vienna University of Technology, 1040 Vienna, Austria*

³ *Russian Quantum Center, Novaya street, 100, Skolkovo, Moscow region 143025, Russia*

⁴ *Institute of Physics and Astrophysics, University of Würzburg, Würzburg, Germany*

(Dated: December 14, 2024)

Starting from the (Hubbard) model of an atom, we demonstrate that the uniqueness of the mapping from the interacting to the noninteracting Green's function, $G \rightarrow G_0$, is strongly violated, by providing numerous explicit examples of different G_0 leading to the same physical G . We argue that there are indeed *infinitely* many such G_0 , with numerous crossings with the physical solution. We show that this rich functional structure is directly related to the divergence of certain classes of (irreducible vertex) diagrams, with important consequences for traditional many-body physics based on diagrammatic expansions. Physically, we ascribe the onset of these highly non-perturbative manifestations to the progressive suppression of the charge susceptibility induced by the formation of local magnetic moments and/or RVB states in strongly correlated electron systems.

PACS numbers: 71.10.-w; 71.27.+a; 71.10.Fd

Introduction. For more than fifty years non-relativistic quantum many-body theory (QMBT) has been successfully applied to describe the physics of many-electron systems in the field of condensed matter. Despite the intrinsic difficulty of identifying a small expansion parameter (analogously to the the fine-structure constant of quantum-electrodynamics), the formalism of QMBT –in its complementary representations in terms of Feynman diagrammatics[1, 2] and of the Luttinger-Ward (LW) functional[3, 4]– is the cornerstone of the microscopic derivation of Landau's Fermi-liquid theory and of uncountable approximation schemes[5–9].

Yet, the actual conditions of applicability of the QMBT in the non-perturbative regime have been scarcely investigated. This is surprising, because QMBT is extensively applied to strongly correlated electron materials, where band-theory and Fermi-liquid predictions fail, and some of the most exotic physics of condensed matter systems is observed. Recently, however, the quest for such investigations became particularly strong. This is because, recently, several cutting-edge QMBT-approaches, explicitly designed for describing the crucial, but elusive, regime of intermediate-to-strong interactions, have been developed or proposed: Among these we recall, e.g., the diagrammatic Quantum Monte Carlo (DQMC) schemes [10] and numerous diagrammatic extensions of dynamical mean field theory (DMFT) [9, 11].

Pioneering analyses of the perturbation theory breakdown have been reported in the last four years[12–21]. The main outcome can be summarized in two independent observations: (i) the occurrence of *infinitely* many singularities in the Bethe-Salpeter equations and (ii) the intrinsic multivaluedness of the LW functionals. The first problem appears as an infinite series of unexpected *divergences* in irreducible vertex functions of correlated electron models[13], while the second is reflected in the convergence of the perturbative series to an un-

physical solution[14]. The intrinsic origin of these non-perturbative manifestations, their impact on the many-electron physics, as well as on the method development in the field, represent a challenge for the current theoretical understanding.

In this Letter, we report a fundamental progress in the comprehension of the perturbation theory breakdown and of its significance. In particular, going beyond the pioneering work of [14], (i) we show that there are many (probably an infinite number of) unphysical self-energies that become equal to the physical one at specific values of the interaction. This puts us into the position to (ii) demonstrate, at the level of the Hubbard atom, the actual correspondence between the *infinitely many* vertex divergences of the Feynman diagrammatics and the occurrence of *infinitely many* bifurcations of the LW functional. Finally, (iii) we generalize these results from the Hubbard atom to generic systems with strong correlations. Regarding the nature of the singularities, we show that vertex divergences of different kinds are reflected in different natures of solution crossings at the bifurcation.

The emerging scenario, which *mathematically* depicts an unexpectedly complex structure of the many-body formalism, will be *physically* related to the progressive suppression of charge fluctuations, a generic property of strongly-correlated systems. The improved understanding of the QMBT beyond the perturbative regime serves as a crucial guidance for future method development for non-relativistic many-electron systems.

Multivaluedness of the Luttinger-Ward functional. The Luttinger-Ward (LW) functional $\Phi[G]$ plays a crucial role in traditional many-body physics [4]. It is a universal functional of the full single-particle Green's function G , which only depends on the electron-electron interaction but not on the external potential. From $\Phi[G]$ the free energy can be determined. One can also obtain the electron self-energy $\Sigma[G] \sim \delta\Phi[G]/\delta G$, entering the Dyson

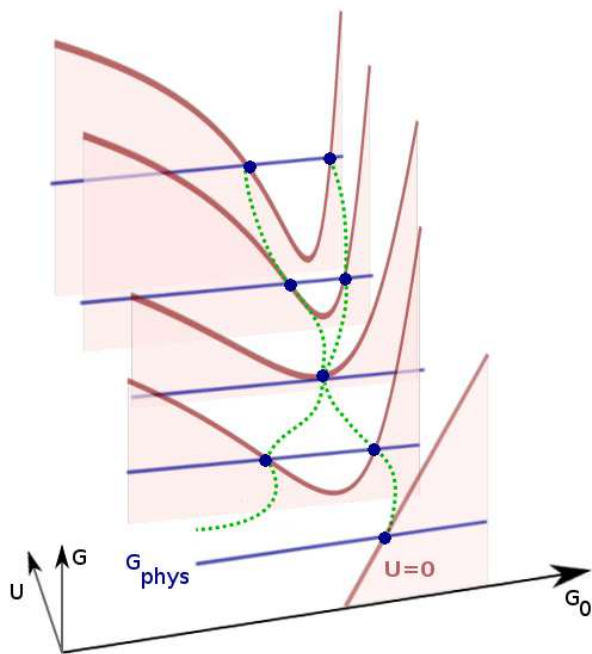


FIG. 1: The relation between the functional $G[G_0, U]$ and G_0 is described by the red curves for different values of U . G and G_0 are here treated as numbers and not functions. The horizontal blue lines show the values of G_{phys} for different U and the blue dots the G_0 which produce G_{phys} .

equation

$$G_0^{-1} - G^{-1} = \Sigma, \quad (1)$$

where G_0 is the noninteracting Green's function determined by the external potential. From $\Sigma[G]$ one can compute all irreducible vertices Γ entering the Bethe-Salpeter equations [8] for response functions. For instance, the charge susceptibility is determined by the vertex [3]

$$\Gamma_c = \frac{\delta \Sigma[G]}{\delta G}, \quad (2)$$

where the explicit index dependence is discussed in Sec. I of the Supplemental Material [22]. Approximations built within this approach are guaranteed to be conserving [3], therefore it is exploited for numerous formal derivations [9, 23–25]. Moreover, the full two-particle nature of the vertices Γ represents an ideal building block for approximations designed to preserve the Pauli principle properties, and related sum rules. In practice, many-body approaches are traditionally built on a limited diagrammatic expansion [2]. For instance, it is believed that the parquet equations [8] are one of the most fundamental ways of performing diagrammatic summations.

In order for QMBT methods to be meaningful, an important property of the functional $G[G_0]$ needs to be fulfilled: The definition of Σ together with the Dyson equation implicitly assumes that there is a unique mapping

between G and G_0 , $G \rightarrow G_0$. Otherwise, several branches of Σ would exist, corresponding to different G_0 , posing the general problem of an intrinsic multivaluedness of any QMBT-based scheme. This is not just a formal issue. If two such branches cross, Γ in Eq. (2) might become ill-defined and diverge. This would challenge important aspects of the traditional many-body theory, such as, e.g., the definition of physically meaningful parquet summations [26].

Fig. 1 schematically illustrates such a scenario. The general functional relation between G and G_0 is depicted by several red curves for different values of the electronic interaction U [27]. G and G_0 are here treated as numbers rather than functions (of frequency/momentum/spin, etc.). For $U = 0$, $G[G_0] = G_0$, and for each physical G (horizontal blue line) the corresponding G_0 is *univocally* determined. When $U > 0$, however, $G[G_0] = G_0$ might not hold anymore and $G[G_0]$ become “wavier”, displaying several maxima/minima in the functional space. This way, the intersection with G_{phys} would correspond to several G_0 (blue dots), of which only one describes the physical system (G_0^{phys}). This formal ambiguity turns into an actual problem, *if* for some values of U the intersection with G_{phys} occurs at one extreme of $G[G_0]$. This would correspond to the intersection of two different solutions of G_0 (and thus of Σ , see green dashed lines in Fig. 1). At this point we would expect $\delta G/\delta G_0 = 0$. Combining this with the Dyson equation and the definition [Eq. (2)] of Γ_c , one would conclude that Γ_c diverges.

To go beyond the sketch of Fig. 1, we present calculations for the Hubbard atom [28] and show that different G_0 indeed do cross for certain values of U . In Sec. IA of the Supplemental Material [22] we then show that such a crossing indeed does lead to divergences of Γ_c .

Method. We have developed a method for finding different G_0 's which lead to the physical G for the Hubbard atom. We use the Hirsch-Fye algorithm [29] to obtain G from a guess for G_0 . This method involves a summation over auxiliary spins, which is usually done stochastically. Here we perform a complete summation using the Gray code [30], thereby avoiding stochastic errors. We guess a G_0 , and then use a Metropolis method to search improved guesses for G_0 . When a promising guess has been found, the Hirsch-Fye equations are repeatedly linearized and solved, until a G_0 has been found which accurately reproduces the physical G (see Sec. II of [22]). It is crucial that there are no stochastic errors in this approach. The method makes it possible to determine if two G_0 really become equal for some U and to determine how they approach each other as U is varied.

Results for the Hubbard atom. Following the presentation in [14], our results are summarized in Fig. 2 (left panel), showing $\text{Tr} \Sigma G_{\text{phys}}/(\beta U)$ as a function of U corresponding to the different G_0 and, hence Σ , via Eq. (1). For $G_0 = G_0^{\text{phys}}$, this quantity yields the double occu-

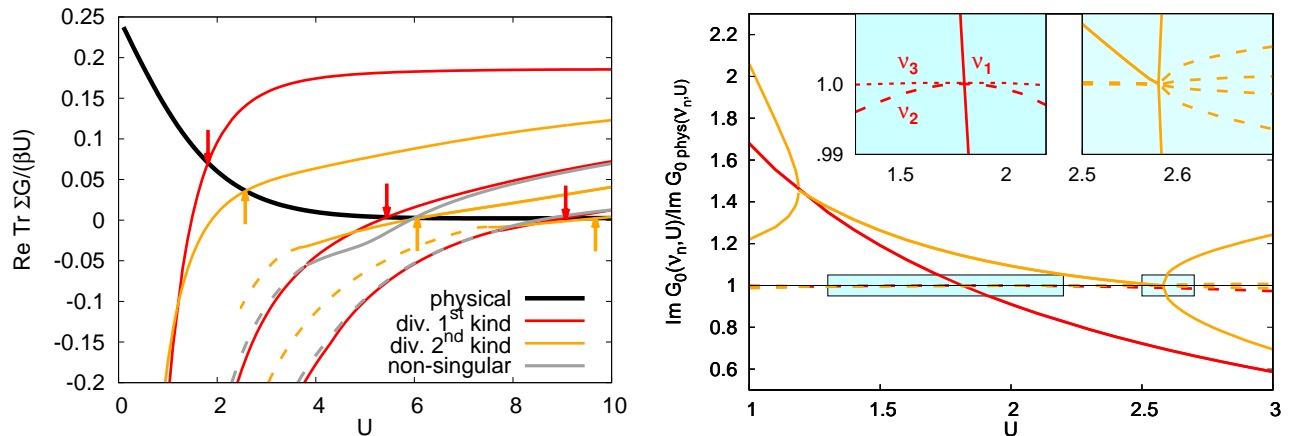


FIG. 2: Left: $\text{Tr } \Sigma G/(\beta U)$ as a function of U corresponding to different G_0 for the Hubbard atom for $\beta = 2$. Red/orange arrows mark the different divergences of Γ_c according to Ref. [13]. The physical curve corresponding to $G_{0\text{phys}}$ is shown in black. At the crossings with the gray curves, $G_0(\nu_n) \neq G_{0\text{phys}}(\nu_n)$, hence no divergence of Γ_c is found (see Sec. IC of the Supplemental Material [22]). Dashed curves indicate that $\text{Tr } \Sigma G/(\beta U)$ also has an imaginary contribution, which is not shown. Right: imaginary part of G_0 (normalized to $\text{Im } G_{0\text{phys}}$) for the first red and orange curves. Results for the absolutely lowest (bold lines), second lowest (dashed lines) and (in insets) third lowest (dotted lines) ν_n are shown.

pancy. The black curve displays the values obtained with $G_0 = G_0^{\text{phys}}$, while the colored (red, orange) curves are the results for the other (unphysical) G_0 , collapsing to G_0^{phys} in the several crossing points shown in the Figure. The latter ones *do* coincide -within our numerical accuracy- with the locations (marked by vertical arrows) of the first six divergences of Γ_c in the Hubbard atom [13]. The red G_0 's are associated to a milder violation of physical relations than the orange ones (e.g., the former can acquire a non-zero real part, but the latter can even violate the generic condition: $G_0(i\nu) = G_0(-i\nu)^*$ [22]). The left red curve was found by Kozik *et al.*[14], although it could not be converged around the crossing with G_0^{phys} .

There are important connections between the frequency dependence of the divergences of Γ_c , coded by red/orange colors [13], and the detailed behavior of G_0 at a crossing. The divergences of Γ_c can be divided in two classes [12, 13]. We consider the generalized charge susceptibility $\chi_c(\nu, \nu', \omega = 0)$ [31], which depends on two fermionic Matsubara frequencies, ν and ν' , and a bosonic frequency $\omega = 0$. Γ_c is then given by

$$\Gamma_c = \beta^2 [\chi_c^{-1} - \chi_{c,0}^{-1}]. \quad (3)$$

Here $\chi_{c,0}$ is the noninteracting generalized susceptibility χ_c , and χ_c and $\chi_{c,0}$ are treated as matrices of ν and ν' . These matrices can be diagonalized

$$\chi_c(\nu, \nu', \omega = 0) = \sum_l V_l(\nu)^* \varepsilon_l V_l(\nu'), \quad (4)$$

with $V_l(\nu)$ and ε_l being the corresponding eigenvectors/-values. While the divergences of Γ_c always correspond to the vanishing of one ε_l , they differ in the frequency-structure of $V_l(\nu)$: For the divergences marked by the red

arrows, $V_l(\nu)$ has only two non-zero elements (at $\pm\nu_n$, with $n = 1, 2, 3, \dots$) reflecting a *localized* divergence at $\nu = \pm\nu_n$, while for the orange arrows, $V_l(\nu) \neq 0 \forall \nu$, reflecting a *global* divergence of Γ_c [13].

An analogous classification is also applicable to the different G_0 resolved in frequency space (see Fig. 2b). In Fig. 2b we plot the ratio $\text{Im } G_0(\nu_n)/\text{Im } G_{0\text{phys}}(\nu_n)$ corresponding to the first two crossings and for the three lowest ν_n . As G_0^{phys} is purely imaginary, the condition $G_0(\nu_n) = G_{0\text{phys}}(\nu_n)$ is reflected in the ratio being unity and $\text{Re } G_0(\nu_n)/\text{Im } G_{0\text{phys}}(\nu_n) = 0$ (shown in Supplemental Material [22]). Fig. 2b demonstrates that the red/orange crossings observed in $\text{Tr } \Sigma G_{\text{phys}}$ indeed corresponds to an actual identity of $G_0(\nu_n) = G_{0\text{phys}}(\nu_n)$, $\forall \nu_n$ both at $U = 1.81$ (red) and 2.58 (orange). Yet, the corresponding zooms in the insets show a *qualitative* difference between the two cases. For the red case, the crossing of G_0 with G_0^{phys} is *linear* in U only for $\nu = \nu_1 = \pi T$ (solid line), while it is $O(U^2)$ for all other ν_n (dashed line). In the orange case, there are linear or even more rapid crossings for all the frequencies shown. As shown in Sec. IA of the Supplemental Material [22], this leads to a divergence of Γ_c for $\nu, \nu' = \pm\nu_1$ for the red crossing and for all frequencies for the orange crossing. Similar results are found for the second and third red and orange crossings, but for the red crossings the linear crossing happens for $\nu_2 = 3\pi/\beta$ (second) and $\nu_3 = 5\pi/\beta$ (third). This is consistent with the result in Ref. [13] that the corresponding divergences of Γ_c happens for these specific ν_n .

The one-to-one correspondence of red/orange crossings with the local/global divergences of Γ_c that we demonstrated for the first six crossings, illustrates how the heuristic scenario of Fig. 1 is actually realized for the

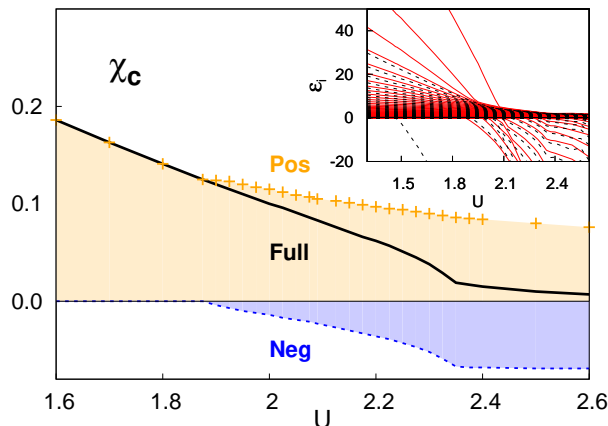


FIG. 3: DMFT calculation of the local charge susceptibility (χ_{ch}) [Eq. (5)] as a function of U for a two-dimensional Hubbard model at half-filling, $\beta = 40$ and $4t = 1$. Both χ_{ch} and its contributions from positive and negative eigenvalues are shown. The inset shows the U -dependence of the eigenvalues ε_i , using solid lines for ε_i with $|\sum_{\nu} V_i(\nu)| > 0$ and dashed lines for the rest.

Hubbard atom. The result also indicates the existence of an *infinite* number of unphysical G_0 , since *infinitely* many red and orange divergences were found for the Hubbard atom [13]. Furthermore, there are indications that the infinity of the total number of G_0 might be of a higher cardinality than that of the vertex divergences, as we discuss in Sec. III of the Supplemental Material [22].

Generic strongly correlated systems. – So far we have discussed the Hubbard atom. To make closer contact to strongly correlated physical systems, we consider the Hubbard model in DMFT [9, 11], where the Hubbard atom is embedded in a self-consistent, noninteracting host. The LW functional is unchanged, since it only depends on the interacting part of the Hamiltonian. The external-potential part, however, changes, and therefore both G_{phys} and G_0^{phys} are different. We can exploit the relation of the crossings with the divergences of Γ_c and the zero eigenvalues in Eq. (4), and gain further insight by analyzing the physical local charge susceptibility. In DMFT, this is given by [26]

$$\chi_{\text{ch}} = \frac{1}{\beta^2} \sum_{\nu, \nu'} \chi_c(\nu, \nu') = \frac{1}{\beta^2} \sum_l \varepsilon_l \left| \sum_{\nu} V_l(\nu) \right|^2. \quad (5)$$

The corresponding DMFT results are reported in Fig. 3. By increasing U , the electrons gradually localize, building up local magnetic moments with longer lifetimes. These, in turn, freeze the local charge dynamics, with χ_{ch} becoming very small especially in the proximity/after the Mott metal-insulator transition (at about $U = 2.3$ for $\beta = 40$). While the physics of this generic trend is known, the projection of χ_{ch} in its eigenvalue-basis yields highly non-trivial information. We analyze χ_{ch} in terms of the contributions from positive and

negative ε_l . For small/moderate U all ε_l are positive. As U increases, one ε_l after the other goes through zero (see inset of Fig. 3). Each time Γ_c diverges [see Eqs. (3, 4)], a new G_0 becomes identical to G_0^{phys} , and the negative component of χ_{ch} becomes more important. Such a negative component of χ_{ch} plays a crucial role in realizing the correct strong coupling physics. Its neglect would lead to a χ_{ch} approximately saturating at some sizable value in the Mott phase, instead of being strongly suppressed. We also note, that a small value of χ_{ch} in itself is not sufficient for this scenario to be realized (e.g., in a dilute system χ_{ch} can be small, but all $\varepsilon_l > 0$). Here, the crucial factor is the mechanism responsible for the freezing of χ_{ch} : the gradual local moment formation which manifests itself in a progressively larger contribution of the negative ε_l . This is, thus, the underlying physics responsible for the occurrence of the (infinitely many) unphysical G_0 crossing G_0^{phys} , and the related divergences of Γ_c . This also applies to the corresponding breakdown of perturbative expansions, such as parquet-based approximations. A certain class of diagrams can give a positive infinite contribution, which is canceled by another class of diagrams [26]. Then the diagrammatic expansion is not absolutely convergent, as was also found in Ref. [14]. This makes conventional diagrammatic expansions highly questionable for intermediate-to-strong correlations. While it is not surprising that perturbative approaches might break down at the Mott transition, it is interesting that this happens well before the Mott transition occurs, where Fermi-liquid physical properties still control the low-energy physics.

It is important to stress that the non-perturbative manifestations discussed in this Letter are affecting not *only* models dominated by purely local physics (such as the Hubbard atom or its DMFT version). In fact, divergences of Γ_c have also been found [26] studying the 2d Hubbard model, by means of the dynamical cluster approximation (DCA) [24]. In this case, the underlying physics behind the change of sign of the ε_l could be related to the formation of an RVB state [32], also responsible [33] for the opening of a spectral pseudogap [34]. One might even expect that increasing the size of the DCA cluster would push the occurrence of the first $\varepsilon_l = 0$ and the pseudogap towards lower U , due to strong antiferromagnetic fluctuation extended on larger length scales [35].

Conclusions. – We reported an important progress towards the understanding of the mathematical structures, which arise in the non-perturbative regime of quantum many body theories, and of the physics behind them. We have demonstrated that the functional space of the LW functionals is even richer than the pioneering results by Kozik *et al.* suggested [14]: At these points, the related two-particle vertex functions display fermionic divergences, of which the multivaluedness of the LW func-

tional can, therefore, be considered as a physical consequence. This can be regarded as formal problem, as long as the unphysical G_0 do not intersect the physical G_0 (as is indeed case in the perturbative regime). However, this is in general *not* true, as many crossings are actually observed, as a result of underlying strong-coupling physical mechanisms at work (i.e., formation of local moments, RVB states, etc.). These crossings are challenging the current quantum many-body algorithms in several respects, being responsible for the divergence of irreducible vertex functions, non-invertibility of the Bethe-Salpeter equations, breakdown of the parquet resummations, etc. For this reason, further investigations of the theoretical foundations beyond the perturbative regime will play a central role for future method developments in condensed matter physics.

Acknowledgments. – We thank S. Ciuchi, P. Thunström, M. Capone, S. Andergassen and K. Held for insightful discussions and P. Chalupa also for carefully reading the manuscript. The authors would like to thank all attendees to the Workshop “Multiple Solutions in Many-Body Theories” held in Paris the 13th and 14th of June 2016 for interesting discussions. We acknowledge support from FWF through the projects I-2794-N35 (TS, AT) and from the research unit FOR 1346 of the DFG (GS).

-
- [1] A. A. Abrikosov, L. P. Gorkov (Autor), F. A. Davis, *Methods of Quantum Field Theory in Statistical Physics* (Dover, New York, 1963).
- [2] A. L. Fetter and J. D. Valecka, *Quantum theory of many-particle systems*, McGraw Hill, New York, 1971.
- [3] G. Baym and L. P. Kadanoff, *Phys. Rev.* **124**, 287 (1961).
- [4] J. M. Luttinger and J. C. Ward, *Phys. Rev.* **118**, 1417 (1960).
- [5] L. Hedin and S. Lundqvist, *Solid State Physics* **23**, 1 (1969).
- [6] N. E. Bickers and D. J. Scalapino, *Phys. Rev. Lett.* **62**, 961 (1989).
- [7] W. Metzner, M. Salmhofer, C. Honerkamp, V. Meden, and K. Schönhammer *Rev. Mod. Phys.* **84**, 299 (2012).
- [8] For a review, see, e.g., N. E. Bickers, *Int. J. Mod. Phys. B* **5**, 253 (1991) and in *Theoretical Methods for Strongly Correlated Electrons*, edited by D. Senechal, A. Tremblay, and C. Bourbonnais (Springer-Verlag, New York, 2004), chapter 6.
- [9] A. Georges, G. Kotliar, W. Krauth, and M. Rozenberg, *Rev. Mod. Phys.* **68**, 13 (1996).
- [10] K. Van Houcke, E. Kozik, N. Prokof'ev, and B. Svistunov, in *Computer Simulation Studies in Condensed Matter Physics XXI*, edited by D. Landau, S. Lewis, and H. Schuttler (Springer Verlag, Berlin, 2008); E. Kozik, K. V. Houcke, E. Gull, L. Pollet, N. Prokof'ev, B. Svistunov, and M. Troyer, *Europhys. Lett.* **90**, 10004 (2010).
- [11] W. Metzner and D. Vollhardt, *Phys. Rev. Lett.* **62**, 324 (1989); M. Jarrell, *Phys. Rev. Lett.* **69**, 168 (1992).
- [12] T. Schäfer, G. Rohringer, O. Gunnarsson, S. Ciuchi, G. Sangiovanni, and A. Toschi, *Phys. Rev. Lett.* **110**, 246405 (2013).
- [13] T. Schäfer, S. Ciuchi, M. Wallerberger, P. Thunström, O. Gunnarsson, G. Sangiovanni, G. Rohringer, and A. Toschi, *Phys. Rev. B* **94**, 235108 (2016).
- [14] E. Kozik, M. Ferrero, and A. Georges, *Phys. Rev. Lett.* **114**, 156402 (2015).
- [15] V. Janiš and V. Pokorny, *Phys. Rev. B* **90**, 045143 (2014).
- [16] T. Ribic, G. Rohringer, and K. Held, *Phys. Rev. B* **93**, 195105 (2016).
- [17] A. Stan, P. Romaniello, S. Rigamonti, L. Reining and J.A. Berger *New J. of Physics* **17** 093045 (2015).
- [18] R. Rossi and F. Werner, *J. Phys. A* **48**, 485202 (2015).
- [19] G. Lani, P. Romaniello, and L. Reining, *New J. Phys.* **14**, 013056 (2012).
- [20] R. Rossi, F. Werner, N. Prokof'ev, and B. Svistunov, *Phys. Rev. B* **93**, 161102(R) (2016).
- [21] W. Tarantino, P. Romaniello, J. A. Berger, and L. Reining, arXiv:1703.05587 (2017).
- [22] Supplemental Material accessible at ...
- [23] J. M. Luttinger, *Phys. Rev.* **124**, 1153 (1960).
- [24] T. Maier, M. Jarrell, T. Pruschke, and M. H. Hettler, *Rev. Mod. Phys.* **77**, 1027 (2005).
- [25] L. Pollet, N. V. Prokof'ev, and B. V. Svistunov, *Phys. Rev. B* **83**, 161103 (2011); S. Biermann, F. Aryasetiawan, and A. Georges, *Phys. Rev. Lett.* **90**, 086402 (2003).
- [26] O. Gunnarsson, T. Schäfer, J.P.F. LeBlanc, J. Merino, G. Sangiovanni, G. Rohringer, and A. Toschi, *Phys. Rev. B* **93**, 245102 (2016).
- [27] Actually, this representation corresponds to the so-called one-point model, see, e.g. [17–20].
- [28] J. Hubbard, *Proc. Roy. Soc. London A* **276**, 238 (1963); M. C. Gutzwiller, *Phys. Rev. Lett.* **10**, 159 (1963); J. Kanamori, *Progr. Theor. Phys.* **30**, 275 (1963).
- [29] J. E. Hirsch and R. M. Fye, *Phys. Rev. Lett.* **56**, 2521 (1986).
- [30] F. Gray, *Pulse code communication*, March 17, 1953 (filed Nov. 1947). U.S. Patent 2,632,058; C. D. Miller, (2000). *Binary Numbers and the Standard Gray Code. Mathematical Ideas (9 ed) Ch. 4* (Addison Wesley Longman, 2000), ISBN 0-321-07607-9.
- [31] G. Rohringer, A. Valli, and A. Toschi, *Phys. Rev. B* **86**, 125114 (2012).
- [32] P. W. Anderson, *Science* **235**, 1196 (1987); S. Liang, B. Doucot, and P. W. Anderson, *Phys. Rev. Lett.* **61**, 365 (1988).
- [33] J. Merino and O. Gunnarsson, *J. Phys.: Cond. Matter. (Fast Track Commun.)* **25**, 052201 (2013); *Phys. Rev. B* **89**, 245130 (2014).
- [34] T. Timusk and B. Statt, *Rep. Prog. Phys.* **62**, 61 (1999).
- [35] T. Schäfer, F. Geles, D. Rost, G. Rohringer, E. Arrighoni, K. Held, N. Blümer, M. Aichhorn, and A. Toschi, *Phys. Rev. B* **91**, 125109 (2015).